Title

Diversification of substrate specificities in teleostei Fads2: Characterization of Δ4 and Δ6Δ5 desaturases of *Chirostoma estor*

Authors

Jorge Fonseca-Madrigal[1], Juan C. Navarro[2], Francisco Hontoria[2], Douglas R. Tocher[3], Carlos A. Martínez-Palacios[1], Óscar Monroig [2,3]*

Running title: Subfunctionalization of teleostei Fads2 desaturases

Addresses

[1] Laboratorio de Acuicultura, Instituto de Investigaciones Agropecuarias y Forestales, UMSNH, Morelia 58330, Michoacán, Mexico

[2] Instituto de Acuicultura Torre de la Sal (IATS-CSIC), Ribera de Cabanes 12595, Castellón, Spain

[3] Institute of Aquaculture, School of Natural Sciences, University of Stirling, Stirling FK9 4LA, Scotland, UK

***Corresponding author**

Dr Óscar Monroig

School of Natural Sciences

University of Stirling

Stirling FK9 4LA, Scotland, UK

Tel. +44 (0)1786 467917

Fax. +44 (0)1786 472133

oscar.monroig@stir.ac.uk

Abbreviations

aa, amino acid

ARA, arachidonic acid (20:4n-6)

BHT, butylated hydroxytoluene

cDNA, complementary DNA

DHA, docosahexaenoic acid (22:6n-3)

Elovl, elongase of very long-chain fatty acids

EFA, essential fatty acids

EPA, eicosapentaenoic acid (20:5n-3)

FA, fatty acid

Fads, fatty acyl desaturase

FAME, fatty acid methyl ester

FID, flame ionization detector

GC-MS, gas chromatography-mass spectrometry

LC-PUFA, long-chain polyunsaturated fatty acids

LNA, α-linolenic acid (18:3n-3)

LOA, linoleic acid (18:2n-6)

OD, optical density

ORF, open reading frame

PCR, polymerase chain reaction

PUFA, polyunsaturated fatty acid

qPCR, quantitative real-time PCR

RACE, rapid amplification of cDNA ends

SCMM, *Saccharomyces cerevisiae* minimal medium

Abstract

Currently existing data show that the capability for long-chain polyunsaturated fatty acids (LC-PUFA) biosynthesis in teleost fish is more diverse than in other vertebrates. Such diversity has been primarily linked to the subfunctionalization that teleostei Fads2 desaturases have undergone during evolution. We previously showed that *Chirostoma estor*, one of the few representatives of freshwater atherinopsids, had the ability for LC-PUFA biosynthesis from C18 PUFA precursors, in agreement with this species having unusually high contents of docosahexaenoic acid. The particular ancestry and pattern of LC-PUFA biosynthesis activity of *C. estor* make this species an excellent model for study to gain further insight into LC-PUFA biosynthetic abilities among teleosts. The present study aimed to characterize cDNA sequences encoding fatty acyl elongases and desaturases, key genes involved in the LC-PUFA biosynthesis. Results showed that *C. estor* expressed an Elovl5 elongase and two Fads2 desaturases displaying Δ4 and Δ6/Δ5 specificities, thus allowing us to conclude that these three genes cover all the enzymatic abilities required for LC-PUFA biosynthesis from C18 PUFA. In addition, the specificities of the *C. estor* Fads2 enabled us to propose potential evolutionary patterns and mechanisms for subfunctionalization of Fads2 among fish lineages.

Supplementary key words

biosynthesis; elongase of very long-chain fatty acids; evolution; fatty acyl desaturases; long-chain polyunsaturated fatty acids; teleosts.

1. Introduction

Biosynthesis of long-chain polyunsaturated fatty acids (LC-PUFA) in vertebrates involves sequential desaturation and elongation of C_{18} PUFA, linoleic acid (LOA; 18:2n-6) and α-linolenic acid (LNA; 18:3n-3) (1). Synthesis of arachidonic acid (ARA; 20:4n-6) and eicosapentaenoic acid (EPA; 20:5n-3) from LOA and LNA, respectively, utilizes the same enzymes and pathways. The predominant pathway involves Δ6 desaturation of LOA or LNA to 18:3n-6/18:4n-3 that are elongated to 20:3n-6/20:4n-3 followed by Δ5 desaturation to ARA/EPA (1), but an alternative pathway with initial elongation of LOA or LNA followed by Δ8 desaturation, an inherent ability of some Δ6 desaturases, may be possible (2). Biosynthesis of docosahexaenoic acid (DHA; 22:6n-3) from EPA can also occur by two pathways. First, the so-called "Sprecher pathway" involves two sequential elongation steps from EPA to 24:5n-3 and a subsequent Δ6 desaturation to 24:6n-3, followed by peroxisomal chain shortening (3). Second, a more direct pathway has been postulated in some marine fish that involves elongation of EPA to docosapentaenoic acid (DPA; 22:5n-3) followed by Δ4 desaturation to DHA (4,5).

Dietary PUFA are essential in fish although requirements vary with species (6,7). Generally, C_{18} PUFA can satisfy essential fatty acid (EFA) requirements of freshwater and salmonid species, but most marine fish have a requirement for LC-PUFA such as EPA and DHA (8). Differing EFA requirements have been linked to differences in the complement of fatty acyl desaturase (Fads) and elongase of very long-chain fatty acid (Elovl) genes (9-31). Thus, the dependence of many marine fish for dietary LC-PUFA was caused by deficiency in key enzymatic activities required for their biosynthesis from C_{18} PUFA (7,8). This was hypothesized to be a consequence of marine fish having evolved in an LC-PUFA-rich environment and thus low evolutionary pressure to retain the ability to desaturate and elongate C_{18} PUFA. In contrast, lower levels of LC-PUFA in the food chain meant freshwater species retained the ability to biosynthesize LC-PUFA from C_{18} PUFA (8,32,33). This

hypothesis was based upon fish that were largely carnivorous in the case of marine species and detritivorous/herbivorous in freshwater species (34). However, trophic level, the position of an organism within the food web, was also investigated and it was demonstrated that the herbivorous marine fish *Siganus canaliculatus* (rabbitfish) had the ability to endogenously synthesize LC-PUFA since two desaturases with Δ4 and Δ6/Δ5 specificities and two elongases (Elovl4 and Elovl5) enabled this species to perform all the enzymatic reactions required in the pathway (4,28). More recently, other confounding factors including "trophic ecology" and diadromy have been proposed (5,30). Currently, data indicate that capability for LC-PUFA biosynthesis in teleost fish is more diverse than in other vertebrate groups, and is possibly the result of a combination of factors that interact throughout the evolutionary history of each particular group or species. Such plasticity has been primarily associated with the substrate specificities exhibited by desaturase Fads2, a protein that has subfunctionalized during evolution of teleosts.

Fads2 has been shown to be the sole Fads-like desaturase existing in teleost genomes, in contrast with other vertebrates that also have another desaturase termed Fads1 (32). Mammalian *FADS1* encodes a desaturase with Δ5 activity, whereas *FADS2* encodes a Δ6 desaturase (35). Consistently, the majority of teleostei Fads2 are typically Δ6 desaturases (11,15,16,21,22,26,27,30). Additionally, however, some teleost Fads2 have been functionally characterized as Δ5 (13), Δ4 (4,5) and bifunctional Δ6/Δ5 (4,9) desaturases. It has been postulated that the reasons underpinning the diversification of Fads2 specificities observed in certain teleost lineages are the result of adaptations to habitat-specific food-web structures in different environments and over geological timescales (32).

Pike silverside *Chirostoma estor* (previously *Menidia estor*) from lake Pátzcuaro is a highly valued freshwater fish in Mexico (36-39). Although *C. estor* is a freshwater species, it has a common ancestry with marine Atherinopsids (40) and shares many biological and physiological characteristics of marine species (41). Also unusually for a freshwater fish,

tissues of *C. estor* show high levels of DHA (20 – 32 % of total fatty acids) and only low levels of EPA (1 – 3 %) in contrast to the fatty acid profile of its zooplankton diet (~ 12 % DHA, 13 % EPA) (42). This suggested that *C. estor* either selectively accumulates DHA, or has the capacity to convert EPA or other n-3 PUFA to DHA (7). Interestingly, the activity of the LC-PUFA synthesis pathway in *C. estor* was very low in freshwater (0 ppt salinity) in comparison to that in higher salinity (5 or 15 ppt), and this was unexpected for a freshwater fish as they generally show appreciable LC-PUFA synthesis activity (43).

The ancestry of *C. estor*, pattern of LC-PUFA biosynthesis activity, and effects of salinity, which conflict with the existing paradigm, made this species an ideal candidate for studies investigating the molecular basis of LC-PUFA biosynthesis to gain further understanding of the diversity that these pathways show among teleost lineages. The objective of the present study was the functional characterization of cDNAs encoding desaturases and elongases involved in the LC-PUFA biosynthetic pathways in *C. estor*. The results indicated that *C. estor* has all the enzymatic capabilities for endogenous biosynthesis of LC-PUFA. In addition to the presence of an Elovl5 elongase, *C. estor* expresses at least two distinct Fads2 enzymes displaying Δ4 and Δ6/Δ5 specificities. The findings on *C. estor* desaturases, provided further insight into the diversification of substrate specificities in teleostei Fads2 and enabled potential evolutionary patterns of subfunctionalized Fads2 among teleost lineages to be proposed.

2. Materials and methods

2.1 Tissue samples

Pike silverside (~40 g) maintained at the facilities of the Instituto de Investigaciones Agropecuarias y Forestales (UMSNH), Mexico, were anaesthetized and sacrificed with an overdose of MS-222 (Sigma-Aldrich, Alcobendas, Spain). Tissues including liver, intestine, brain and muscle were collected in RNAlater (Ambion, Applied Biosystems, Warrington,

UK) according to manufacturer's instructions. Fish maintenance and sacrifice procedures were carried out in compliance with the Official Mexican Standard NOM-062-ZOO-1999 on "Technical specifications for production, care and use of laboratory animals". This study was also reviewed and approved by the departmental Ethics Committees of Institute of Aquaculture Torre de la Sal (CSIC, Spain) and Institute of Aquaculture (University of Stirling, UK).

2.2 Cloning of fatty acyl desaturases and elongase from C. estor

Total RNA (2 µg) extracted from *C. estor* tissues (TRI Reagent, Sigma-Aldrich) was reverse transcribed using a GoScript™ Reverse Transcription System (Promega, Madison, WI, USA) primed with random primers. The primers UNIDF (5'-GGAGAGGAYGCCACGGAGG-3') and UNIDR (5'- GTCCRCTGAACCAGTCGTTGAA-3') for *fads2*, and UNIE5F (5'- CATGGATGGGYCCMAGAGATC-3') and UNIE5R (5'-GTCTGAATGTAGAAGTTTGAGAAAAG-3') for *elovl5* were used to amplify a partial fragment of these genes from *C. estor* by polymerase chain reaction (PCR) with GoTaq® Green Master Mix (Promega) as described previously (30). A mixture of cDNA from liver and brain and was used as template for PCR, which consisted of an initial denaturing step at 95 ºC for 2 min, followed by 40 cycles of denaturation at 95 ºC for 30 s, annealing at 50 ºC for 30 s, extension at 72 ºC for 1 min 30 s, followed by a final extension at 72 ºC for 5 min. The PCR fragments were purified and sequenced at the DNA Sequencing Service IBMCP-UPV (Valencia, Spain). While one single version of the *elovl5*-like cDNA sequence was detected, sequencing results of the desaturase-targeted PCR revealed the existence of at least two distinct *fads2*-like transcripts. Their individual sequences, thereafter referred to as Fads2a and Fads2b, were determined after ligation of the PCR product into pGEM-T Easy vector (Promega) and sequencing as above. The partial sequences within the open reading frame (ORF) of the two desaturases and the elongase were further extended by 5' and 3' rapid

amplification of cDNA ends (RACE) PCR (FirstChoice® RLM-RACE kit, Ambion) through a two-round (nested) PCR approach as detailed below (see supplementary Table 1 for primer details).

For desaturase Fads2a, first round PCR was performed combining the adapter-specific 5'RACE OUTER primer with the gene-specific reverse primer CEFaR1, whose 3' end sequence contained two nucleotides that differ from the Fads2b sequence. A second round PCR with 5'RACE INNER primer and CEFaR2 produced a positive band expanding out the putative end of the 5'UTR. For the Fads2b cDNA sequence, a specific 5'RACE product was not obtained, but the ORF of *fads2b* was obtained to enable functional characterization as detailed below.

Positive 3'RACE PCR products were obtained using isoform-specific primers and 3' adapter primers. First round PCR involved the use of forward primers CEFaF1 (isoform a) and CEFbF1 (isoform b) with the 3'RACE OUTER primer. First round products were subsequently used as template for nested PCR with forward primers CEFaF2 (isoform a) and CEFbF2 (isoform b), with reverse primers consisting of the adapter primer 3'RACE INNER.

A similar approach was followed to obtain the full-length cDNA of *C. estor elovl5*. The gene-specific primers CEE5R1 and CEE5R2 (5' RACE) and CEE5F1 and CEE5F2 (3'RACE) used for RACE PCR are listed in supplementary Table 1. General RACE PCR conditions consisted of an initial denaturing step at 95 ºC for 2 min, followed by 32-35 cycles of denaturation at 95 ºC for 30 s, annealing at 55-60 ºC for 30 s, extension at 72 ºC for 2 min 30 s, followed by a final extension at 72 ºC for 5 min (GoTaq® Green Master Mix, Promega). PCR products were cloned into pGEM-T Easy Vector (Promega) and sequenced as above.

2.3 Sequence and phylogenetic analyses

The amino acid (aa) sequences of the *C. estor* desaturases Fads2a and Fads2b, and elongase Elovl5 proteins were compared to those of orthologues from other fish and tetrapods

(mammals, amphibians and birds) and sequence identity scores were obtained using the EMBOSS Needle Pairwise Sequence Alignment tool (http://www.ebi.ac.uk/Tools/psa/emboss_needle/). For phylogenetic analysis of the *C. estor* deduced aa sequences of *fads2a, fads2b* and *elovl5*, two trees were constructed using the neighbor-joining method (44), with confidence in the resulting tree branch topology measured by bootstrapping through 10,000 iterations. Desaturase and elongase *C. estor* sequences were compared to homologous proteins from a variety of vertebrate lineages. The Δ6 desaturase and the PUFA elongase sequences from the oleaginous fungus *Mortierella alpina* were used as outgroup sequences to construct both rooted trees.

2.4 Functional characterization of the C. estor Fads2 and Elovl5 by heterologous expression in yeast

PCR fragments corresponding to the ORF of pike silverside desaturases *fads2a* and *fads2b* and elongase *elovl5* were amplified from a mixture of cDNA (liver and brain) by PCR using the high fidelity *Pfu* DNA Polymerase (Promega) with primers containing *Hin*dIII and *Sac*I restriction sites (underlined in supplementary Table I) as follows. For *fads2a*, the primer pair CEFVF-CEFaVR was used. For *fads2b*, the same forward primer CEFVF and the antisense primer CEFbVR were used. While CEFVF was specific for both isoforms, its use in combination with the *fads2b* specific primer CEFbVR enabled us to successfully isolate *fads2b*. Finally, the ORF of the *elovl5* was isolated using the primers CEE5VF and CEE5VR (supplementary Table I). PCR consisted of an initial denaturing step at 95 ºC for 2 min, followed by 35 cycles of denaturation at 95ºC for 30 s, annealing at 57 ºC for 30 s, extension at 72 ºC for 3 min (desaturase) or 2 min (elongase), followed by a final extension at 72 ºC for 5 min. The PCR products were subsequently purified (Illustra GFX PCR DNA/Gel Band Purification Kit, GE Healthcare, Little Chalfont, UK), digested with the corresponding restriction enzymes (Promega) and ligated into a similarly restricted pYES2 yeast expression

vector (Invitrogen, Paisley, UK). The plasmid constructs prepared were designated as pYES2-fads2a, pYES2-fads2b and pYES2-elovl5.

Yeast competent cells InvSc1 (Invitrogen) were transformed with the desaturase (pYES2-fads2a, pYES2-fads2b) and elongase (pYES2-elovl5) plasmid constructs and then grown in selective *S. cerevisiae* minimal medium (SCMM)-^{uracil} medium (10). A single recombinant colony for each enzyme was grown in SCMM-^{uracil} broth and diluted to OD600 of 0.4 in one single Erlenmeyer flask for each potential substrate assayed. The substrate specificities of both *fads2* isoforms were assessed by growing the transgenic yeast in medium supplemented with one of the following substrates: 18:3n-3 or 18:2n-6 for Δ6 desaturation, 20:3n-3 or 20:2n-6 for Δ8 desaturation, 20:4n-3 or 20:3n-6 for Δ5 desaturation, and 22:5n-3 or 22:4n-6 for Δ4 desaturation. The function of *C. estor* Elovl5 was characterized by growing yeast transformed with pYES2-elovl5 in medium containing one of the following PUFA substrates: 18:3n-3, 18:2n-6, 18:4n-3, 18:3n-6, 20:5n-3, 20:4n-6, 22:5n-3 and 22:4n-6. The fatty acid (FA) substrates were added to the yeast cultures at final concentrations of 0.5 (C_{18}), 0.75 (C_{20}) and 1.0 (C_{22}) mM to compensate for decreased efficiency of uptake with increased chain length (19). Yeast transformed with empty pYES2 were also grown in presence of PUFA substrates as control treatments. After 2-days culture at 30 ^{o}C, yeast were harvested, washed, and total lipid extracted by homogenization in chloroform/methanol (2:1, v/v) containing 0.01% butylated hydroxytoluene (BHT) as antioxidant. Results were confirmed by running the assay with a different transformant colony.

All PUFA substrates, except stearidonic acid (18:4n-3), were from Nu-Chek Prep, Inc (Elysian, MN, USA). Stearidonic acid and chemicals used to prepare *S. cerevisiae* minimal medium-^{uracil} were from Sigma-Aldrich, except for the bacteriological agar obtained from Oxoid Ltd. (Hants, UK).

2.5 Fatty acid analysis of yeast

Total lipids were extracted from yeast samples and fatty acyl methyl esters (FAME) were prepared as described previously (9,30). FAME were quantified using a Thermo Gas cChromatograph (Thermo Trace GC Ultra, Thermo Electron Corporation, Waltham, MA, USA) fitted with an on-column injection system and a FID detector. Additionally, FAME were identified using an Agilent 6850 Gas Chromatograph system coupled to a 5975 series MSD (Agilent Technologies, Santa Clara, CA, USA). The desaturation or elongation conversion efficiencies from exogenously added PUFA substrates were calculated by the proportion of substrate FA converted to desaturated or elongated products as [individual product area/(all products areas + substrate area)] x 100. For the elongase, some of the initial elongation products were further elongated and thus the accumulated conversions were calculated by summing all elongated products (28). Similarly, the desaturase Fads2b exhibited multifunctional abilities and thus the conversions on Δ8 substrates (20:3n-3 and 20:2n-6) include stepwise reactions.

2.6 Tissue distribution of fads2 and elovl5 transcripts

Expression of the target genes (*fads2a*, *fads2b* and *elovl5*) was measured by quantitative real-time PCR (qPCR). Total RNA from liver, brain, intestine and muscle was extracted from three *C. estor* adult individuals as described above, and 2 µg of total RNA were reverse transcribed into cDNA (M-MLV reverse transcriptase, Promega) using oligo-dT primer. The qPCR was performed using primers shown in supplementary Table I. Copy numbers of target genes were normalized with copy number of the reference gene *ef-1α* (GenBank accession number KJ439615). PCR amplicons of each gene were cloned into pGEM-T Easy vector (Promega) that was then linearized, quantified spectrophotometrically (NanoDrop 2000c, Thermo Scientific, Wilmington, USA) and serial-diluted to generate a standard curve of known copy numbers. The qPCR amplifications were carried out in duplicate using a CFX96 BioRad machine (Alcobendas, Spain) in a final volume of 20 µl containing 5 µl diluted (1/20)

cDNA, 0.25 µM of each primer and 4 µl PyroTaq EvaGreen® mix (Cultek Molecular Bioline, Madrid, Spain). Amplifications were carried out with a systematic negative control (NTC: no template control) containing no cDNA. The qPCR profiles consisted of an initial activation step at 95 °C for 15 min, followed by 40 cycles of 15 s at 95 °C, 20 s at the specific primer pair annealing Tm (supplementary Table I) and 15 s at 72 °C. After the amplification phase, a dissociation curve of 0.5 °C increments from 60 to 90 °C was performed, enabling confirmation of the amplification of a single product in each reaction. No primer-dimer formation occurred in the NTC. All reactions were carried out in duplicate and a linear standard curve was drawn, and the absolute copy number of the targeted gene in each sample was calculated.

2.7 Statistical analysis

Tissue expression (qPCR) results were expressed as mean normalized values (± SE) corresponding to the ratio between the copy numbers of *fads2a*, *fads2b* and *elovl5* transcripts and the copy numbers of the reference gene *ef-1α*. A one-way analysis of variance (ANOVA) followed by Tukey HSD test ($P<0.05$) was performed to compare the expression level among the selected tissues (SPSS, Chicago, USA).

3. Results

3.1 C. estor fads2 and elovl5 sequences and phylogenetics

Both pike silverside *fads2* desaturases (a and b) have an ORF of 1,326 bp encoding putative proteins of 441 aa that are 88.4 % identical to each other. Pairwise aa sequence comparisons of *C. estor* Fads2 proteins and other homologs from fish (*Cyprinus carpio, Siganus canaliculatus, Danio rerio, Solea senegalensis, Argyrosomus regius, Psetta maxima, Lates carcarifer, Rachycentron canadum, Salmo salar*) showed identities ranging from 68.1 to 82.1 %, with mammalian FADS2 (*Homo sapiens, Mus musculus, Rattus norvegicus*) ranging from

63.3 to 65.5 %. Lower identity scores were obtained with other desaturase families from mammals (*H. sapiens, M. musculus, R. norvegicus*), namely FADS1 (56.2-58.2 % identity) and FADS3 (51.8-55.5 %). Sequence comparison of the *C. estor* Fads2a with the Δ4 desaturase from *Thraustochytrium* sp. ATCC21685 (45) resulted in 22.7 % identity. Analysis of the deduced aa sequence of *C. estor* clones revealed that they had structural features of fatty acyl desaturases including three histidine boxes (HDFGH, HFQHH and QIEHH) and a putative cytochrome b5-like domain in the N-terminus containing the typical HPGG motif essential for desaturation activity (35). GenBank accession numbers for the newly cloned cDNA sequences are KJ417838 (*fads2_a*) and KJ417839 (*fads2_b*).

The ORF of the *C. estor elovl5* was 885 bp long, encoding a protein of 294 aa. Pairwise comparison of the translated aa sequence showed that the Elovl5 shared 81.1-67.7 % identity to Elovl5 proteins from fish (*D. rerio, A. regius, C. striata*, *L. calcarifer* and *S. aurata*), and 62.5 % to that from *H. sapiens*, 62.7 % to that from *Xenopus tropicalis* and 64.4 % to that of *Gallus gallus*. Lower identities (38.0-52.3 %) were obtained when the *C. estor* Elovl5 was compared to other elongase families such as Elovl2 and Elovl4 from different vertebrate lineages including teleosts, amphibians, birds and mammals. The *C. estor* Elovl5 had a diagnostic histidine box (HVYHH), and lysine (K) and arginine (R) residues at the carboxyl terminus (KKLRVD). The sequence of the *elovl5* cDNA from *C. estor* was deposited in GenBank with accession number KJ417837.

Phylogenetic trees constructed on the basis of aa sequence comparisons of the *C. estor* cDNAs with homologous proteins from fish and other vertebrate species reflected the identity scores shown above. For desaturases, the *C. estor* Fads2 clustered with Fads2 from fish and more distantly with Fads2 from mammals, bird and amphibians (Fig. 1). Additionally, Fads1-like proteins, a "front-end" desaturase not present in teleost fish (32), grouped separately from the Fads2 cluster that included the *C. estor* desaturases (Fig. 1). On the other hand, the *C. estor* Elovl5 grouped together with other teleost and tetrapod (mammals, birds and

amphibians) orthologues, and separately from members of Elovl2 and Elovl4 families from fish and other vertebrates (Fig. 2).

3.2 Functional characterization in yeast

The ORF of *C. estor* desaturases Fads2a and Fads2b, along with the elongase Elovl5 were functionally characterized in yeast. Control treatments, consisting of yeast transformed with empty pYES2 vector, indicated there was no endogenous activity as all exogenously added PUFA substrates remained unmodified. Hence, the FA profile of control yeast was characterized by the main endogenous FA of *S. cerevisiae*, namely 16:0, 16:1 isomers (16:1n-9 and 16:1n-7), 18:0, 18:1 isomers (18:1n-9 and 18:1n-7) (22), plus the exogenously added PUFA (data not shown). This indicated that wild-type yeast do not express activities towards PUFA substrates, in agreement with earlier observations (9,10). Yeast expressing the *C. estor* desaturases and elongases showed additional peaks. Yeast transformed with pYES2-fads2a and grown in the presence of 22:5n-3 and 22:4n-6 showed additional peaks corresponding to 22:6n-3 and 22:5n-3, respectively, with identities confirmed by GC-MS (Fig. 3). The conversions of these desaturation reactions are shown in Table I. These results confirmed that Fads2a from *C. estor* had Δ4 desaturase activity. Moreover, the *C. estor* Fads2a exhibited some Δ5 activity on 20:4n-3 that was desaturated to 20:5n-3, although no Δ5 desaturation was detected towards 20:3n-6 (Table 1).

In spite of its homology with the Fads2a aa sequence, the *C. estor* Fads2b showed a remarkably different pattern of FA substrate specificity. Whereas no Δ4 desaturation was detected, Fads2b conferred on yeast the ability to desaturate both Δ6 substrates 18:3n-3 and 18:2n-6 to 18:4n-3 and 18:3n-6, respectively, and Δ5 substrates 20:4n-3 and 20:3n-6 to 20:5n-3 and 20:4n-6, respectively (Fig 3; Table 1), which indicated the *C. estor* Fads2b had dual Δ6Δ5 activity. Conversions obtained from the yeast assays suggested that both *C. estor* Fads2 enzymes more efficiently desaturated n-3 than n-6 PUFA when each homologous pair of

substrates for Δ6- (18:3n-3 and 18:2n-6), Δ5- (20:4n-3 and 20:3n-6) and Δ4-desaturase (22:5n-3 and 22:4n-6) were compared (Table 1).

The inherent capability of vertebrate Fads2 enzymes for Δ8 desaturation was investigated in both isoforms. Only Fads2b exhibited the ability to desaturate 20:3n-3 and 20:2n-6 to the corresponding Δ8-desaturated products 20:4n-3 and 20:3n-6, respectively (Table 1). The relative Δ6/Δ8 activity ratio for Fads2b towards n-3 substrates (18:3n-3 *vs*. 20:3n-3 conversion) was 4.6. Interestingly, the products of Δ8 desaturation, 20:4n-3 and 20:3n-6, were further desaturated to 20:5n-3 and 20:4n-6, respectively, confirming the Δ5 desaturase activity of the enzyme (Fig. 4; Table 1). For 20:3n-3, direct desaturation of 20:3n-3 as Δ6 or Δ5 led to the production of minor peaks identified by GC-MS as non-methylene-interrupted products $^{\Delta 6,11,14,17}$20:4 or $^{\Delta 5,11,14,17}$20:4 (Fig. 4).

The *C. estor* elongase exhibited FA substrate specificities consistent with those of Elovl5 enzymes. Thus, transgenic yeast expressing the coding sequence of the pike silverside *elovl5* showed activity towards most of the PUFA substrates assayed, with particularly high conversions for most C_{18} and C_{20} substrates. Among C_{18} substrates, high elongations were obtained with 18:3n-3, 18:4n-3 and 18:3n-6, which were converted to the corresponding C_{20} products 20:3n-3, 20:4n-3 and 20:3n-6, respectively (Table 2). Further elongations to C_{22} secondary products could be detected in yeast incubated with 18:3n-3, 18:2n-6 and 18:4n-3. For C_{20} PUFA substrates, almost 90 % of total EPA was elongated to 22:5n-3, whereas ARA was elongated to 22:4n-6 to a lower extent (54.8 %). C_{22} PUFA substrates including 22:5n-3 and 22:4n-6 were only marginally or not converted to longer products (Table 2; Fig. 5). For each pair of homologous substrates considered, conversions obtained from the yeast assays suggested that the *C. estor* Elovl5 more efficiently elongated n-3 than n-6 PUFA on a consistent basis (Table 2). Thus, 18:3n-3, 18:4n-3 and 20:5n-3 were elongated to a greater extent than the corresponding n-6 PUFA substrates 18:2n-6, 18:3n-6, 20:4n-6, respectively.

Particularly interesting was the difference in the conversions observed between 18:3n-3 (up to 41.1 % converted to longer products) and 18:2n-6 (only 5.5 % converted to longer products).

3.3 Tissue distribution of fads2 and elovl5 transcripts

Tissue distribution of the *C. estor fads2* (a and b isoforms) and *elovl5* mRNA in adult specimens was analyzed by qPCR. Both *fads2* transcripts were detected in all four tissues analyzed, with significantly higher expression signals found in liver compared to brain, intestine and muscle (Fig. 6). With regards to *elovl5*, liver also showed the highest expression rates, but significant differences could only be established with brain and muscle signals (Fig. 6).

4. Discussion

A previous study suggested that *C. estor* had an active LC-PUFA biosynthesis pathway that enabled this species to endogenously synthesize DHA from PUFA precursors (43). Here, we provide robust data supporting a likely molecular mechanism demonstrating that *C. estor* expresses genes encoding enzymatic activities that would enable the synthesis of DHA.

The capabilities exhibited by the two desaturase cDNAs cloned from *C. estor* (Fads2a and Fads2b) cover the set of desaturation requirements for DHA synthesis from LNA (18:3n-3). Heterologous expression of Fads2b showed this protein was a dual Δ6Δ5 desaturase and thus it catalyzed the desaturation of 18:3n-3 to 18:4n-3 (Δ6) and also the Δ5 desaturation required to convert 20:4n-3 to EPA. While the *C. estor* Fads2a can partly contribute to the Δ5 desaturation leading to EPA biosynthesis as described for Fads2b, the higher conversion activities of Fads2a suggested that its major role in the overall pathway was to catalyze the Δ4 desaturation involved in the direct conversion of 22:5n-3 to DHA. A similar pathway of DHA biosynthesis from EPA was postulated to operate in the rabbitfish *S. canaliculatus* (4,28) and more recently Senegalese sole *S. senegalensis* (5). In comparison with the Sprecher pathway,

the so-called "Δ4 pathway" is a more direct metabolic route as it avoids translocation of PUFA intermediates (namely 24:6n-3) between endoplasmic reticulum and peroxisomes, and also the further catabolic step (partial oxidation to DHA) occurring in the latter organelle (3,46). While we did not test the ability of *C. estor* desaturases to mediate the Δ6-desaturation of 24:5n-3 to 24:6n-3 required in the Sprecher pathway, we hypothesize that it is not operative in the presence of a more direct and efficient mechanism such as the Δ4 pathway. In agreement, neither hepatocytes nor enterocytes of *C. estor* that had been incubated with either [1-^{14}C]-18:3n-3 or [1-^{14}C]-20:5n-3 showed any recovery of radioactivity in Sprecher pathway intermediates, namely 24:5n-3 to 24:6n-3 (43). Moreover, the functional characterization of the *C. estor* Elovl5 supports such a hypothesis.

The Elovl5 of *C. estor* showed virtually no ability to elongate 22:5n-3 to 24:5n-3 as would be required in the Sprecher pathway. This is in agreement with the great majority of fish Elovl5, with the exception of orthologs from rabbitfish (10.6 % conversion from 22:5n-3 to 24:5n-3) (28) and, to a lesser extent, cobia (6.6 % conversion) (19). Also consistent with Elovl5 from fish, the *C. estor* Elovl5 showed substantial activity for the elongation of C_{18} and C_{20} PUFA to the corresponding C_{20} and C_{22} PUFA products, including the elongations of 18:4n-3 to 20:4n-3 and 20:5n-3 to 22:5n-3, which were catalyzed in yeast at high conversions (60.2 and 89.6 %, respectively). Clearly, the *C. estor* Elovl5 can support all the elongation reactions required for DHA biosynthesis through the Δ4 pathway. Taken together, the functional characterization data for Elovl5, Fads2a and Fads2b, and the biochemical assays with radiolabelled PUFA substrates (43), predicts a putative pathway of biosynthesis of LC-PUFA in *C. estor* from dietary essential C_{18} PUFA, 18:3n-3 and 18:2n-6 (Fig. 7). In addition to the DHA biosynthetic pathway described above, two possible pathways for EPA and ARA biosynthesis are shown. First, the "classical", and likely the most prominent, pathway involving Δ6 desaturation – elongation – Δ5 desaturation is possible through the consecutive action of Fads2b, Elovl5 and Fads2b, respectively. Second, the alternative "Δ8 pathway"

proceeds through an initial elongation of dietary essential C_{18} PUFA by Elovl5, followed by two consecutive desaturations catalyzed by Fads2b, first as Δ8 and second as Δ5 (Fig. 7). The *C. estor* Elovl5 was effective in elongating both 18:3n-3 and 18:2n-6 as required in the Δ8 pathway, elongase abilities previously demonstrated in Elovl5 from Southern bluefin tuna (20) and meagre (30). Moreover, the desaturase activities required for the Δ8 pathway, namely Δ8 and Δ5, were demonstrated by Fads2b, but not Fads2a. While the activity of Fads2a as Δ4-desaturase suggested a steric impediment disabling the insertion of new double bonds at Δ6 or Δ8 positions, the Fads2b desaturase showed the ability to desaturate both 20:3n-3 and 20:2n-6 at the Δ8 carbon.

The ability of fish Fads2 to catalyze Δ8 desaturation has been regarded as a characteristic primarily of marine species, and thus relatively low values of Δ6/Δ8 ratio, i.e. the ratio of the conversions towards 18:3n−3 and 20:3n−3, are shown by Fads2 from species of marine origin (2). The Δ6/Δ8 of the *C. estor* Fads2b was 4.6, slightly above the range of Δ6/Δ8 ratios of marine fish desaturases (1.8–4.2), but well below those of desaturases from salmonid/freshwater species (12.0–91.2) (2). Moreover, the activities of the LC-PUFA biosynthetic pathways measured in hepatocyte and enterocyte primary cultures from *C. estor* (40) were generally lower than those obtained in Atlantic salmon (47), but higher than those obtained in the marine teleost Atlantic cod (*Gadus morhua*) (15). Interestingly, the tissue distribution of the desaturases and elongases generally reflected a “freshwater fish” pattern for *C. estor*. Thus, liver had the highest mRNA levels for both desaturases and the elongase and appeared as a major metabolic site for LC-PUFA biosynthesis, over intestine, brain and muscle. Consistently with the mRNA tissue distribution data, previous studies highlighted the unusually high contents of DHA in *C. estor* liver, brain and muscle, and also other tissues including gonads and adipose tissues (38). Similar tissue distribution patterns were observed in freshwater/salmonid species including Atlantic salmon (14,18) and zebrafish (17), in which liver and intestine exhibited highest expression signals of *fads2* and *elovl2* and *elovl5*

elongase genes. Marine fish species including Asian sea bass, Atlantic cod and cobia had the highest expression levels of LC-PUFA biosynthesis genes in brain (15,19,21). The relatively low Δ6/Δ8 ratio of Fads2b, which was typical of marine species on one hand, and the higher expression of desaturase/elongase mRNA in liver, which was typical of freshwater species on the other, probably reflected the particular evolutionary history of *C. estor*. Therefore, while *C. estor* shares some "marine" features with most of its atherinopsid counterparts, it also reflects some characteristics typically found in freshwater species (42).

The substrate specificities of *C. estor* desaturases described here are not entirely unique among fish Fads2 enzymes and, as mentioned above, similar substrate specificities (Δ4 and Δ6Δ5) were found in two desaturases isolated from rabbitfish (4). Furthermore, a Δ6Δ5 Fads2 and a Δ4 Fads2 were previously identified from zebrafish (9) and Senegalese sole (5), respectively, and a monofunctional Δ5-Fads2 was also cloned from Atlantic salmon (13). Provided the gnathostomata (jawed fish) ancestral Fads2 had Δ6-desaturase activity (32) as for mammalian FADS2 (35), the expansion of Fads2 in teleosts has been accompanied by subfunctionalization in the enzyme derived from independent mutations in the primary aa sequence (32). Although a recent study identified a single aa residue as determining the differential ability for 22:5n-3 elongation between ELOVL2 and ELOVL5 elongases in rat (48), identification of specific domains/residues controlling the functionality of desaturases has been elusive and studies are restricted to non-vertebrate enzymes (49-51).

However, the above said, the existence of three Δ6Δ5 desaturases and three Δ4 desaturases distributed in four distinct species, allows us to explore potential evolutionary scenarios for teleostei Fads2 subfunctionalization. The recently revised tree of life of bony fish (52), based on 369 families, allows us to investigate whether the diversity of substrate specificities of *C. estor* desaturases can be related in an evolutionary context along with those of other desaturases with Δ4 and Δ6Δ5 activities previously described from *S. canaliculatus* (4), *S. senegalensis* (5) and *D. rerio* (9). The three species possessing a Δ4 desaturase (*S.*

canaliculatus, *S. senegalensis* and *C. estor*) belong to three different clades including Percomorpharia (*S. canaliculatus*), Carangimorphariae (*S. senegalensis*) and Ovalentariae (*C. estor*), all sharing a common ancestor (~115 Ma). It is tempting to speculate that Fads2 enzymes in fish with Δ4 activity are restricted to these three groups, albeit these groups contain > 200 families and so the activity is likely further restricted to specific families or even individual species within the groups. Thus, other species within these three groups including *A. regius*, *T. thynnus*, *L. calcarifer*, *D. labrax*, *S. aurata*, *R. canadum* (Percomorpharia), *Psetta maxima* (Carangimorphariae) and *Oreochromis niloticus* (Ovalentariae) have Fads2 enzymes functionally characterized as Δ6 desaturases (11,16,19,21,26,27,29,30). However, investigation of desaturases from representatives of other phylogenetic branches is required to confirm this hypothesis.

Establishing a potential pattern of distribution for Fads2 enzymes in teleost fish lineages showing Δ6Δ5 activity is more speculative as the three species displaying these activities (*D. rerio*, *S. canaliculatus* and *C. estor*) are more distantly related. While the groups of *C. estor* and *S. canaliculatus* are relatively close and thus the presence of Δ6Δ5 Fads2 might have a similar restricted evolutionary context as described for Δ4 desaturases, the existence of a dual Δ6Δ5 desaturase in *D. rerio*, belonging to the more ancient cyprinid lineage, does not follow common evolutionary patterns, although it is possible that convergent evolution may have occurred. Assuming the ancient Fads2 was a Δ6 desaturase (32), subfunctionalization of some Fads2 in distantly related lineages (cyprinids *vs.* atherinopsids and siganids) led to the acquisition of Δ5 desaturase activity possibly through discrete mutations at the catalytic site. According to the proposed time-calibrated tree, the emergence of the dual Δ6Δ5 in cyprinids occurred ~100 Ma ago (52), as the desaturase from common carp (also cyprinid) does not show dual activity.

In summary the present study demonstrated that *C. estor* expresses desaturase and elongase genes encoding all the enzymatic activities required for the biosynthesis of DHA from the C_{18}

precursor LNA. While the *C. estor* Elovl5 accounted for all the elongation steps, two distinct Fads2-like desaturase enzymes displaying Δ4 and Δ6Δ5 specificities operate along the pathway. More importantly, the uncommon substrate specificities of Fads2 from *C. estor* and other species like *D. rerio*, *S. canliculatus* and *S. senegalensis* enabled us to propose potential evolutionary scenarios that explain the distribution of such subfunctionalized Fads2 among fish lineages.

5. Acknowledgements

This study and OM were supported by a Marie Curie Reintegration Grant within the 7th European Community Framework Programme (PERG08-GA-2010-276916, LONGFA). Additional funding was obtained from CONACYT, Mexico (INSAM FOINS 102/2012) and from the Ministry of Science and Innovation (Spanish Government) through the OCTOPHYS Project (AGL-2010-22120-C03-02).

6. Disclosures

The authors have no conflict of interest related to this work.

7. References

1 Cook, H.W., and R.C.R. McMaster. 2004. Fatty acid desaturation and chain elongation in eukaryotes. *In* Biochemistry of Lipids, Lipoproteins and Membranes. D.E. Vance and J.E. Vance, editors. Elsevier, Amsterdam. 181–204.

2 Monroig, Ó., Y. Li and D.R. Tocher. 2011. Delta-8 desaturation activity varies among fatty acyl desaturases of teleost fish: high activity in delta-6 desaturases of marine species. *Comp. Biochem. Physiol.* **159***B*: 206-213.

3 Sprecher, H. 2000. Metabolism of highly unsaturated n-3 and n-6 fatty acids. *Biochim. Biophys. Acta* **1486**: 219-231.

4 Li, Y., Ó. Monroig, L. Zhang, S. Wang, X. Zheng, J.R. Dick, C. You and D.R. Tocher. 2010. Vertebrate fatty acyl desaturase with Δ4 activity. *Proc. Natl. Acad. Sci. USA* **107**: 16840-16845.

5 Morais, S., F. Castanheira, L. Martínez-Rubio, L.E.C. Conceição and D.R. Tocher. 2012. Long-chain polyunsaturated fatty acid synthesis in a marine vertebrate: ontogenetic and nutritional regulation of a fatty acyl desaturase with Δ4 activity. *Biochim. Biophys. Acta* **1821**: 660-671.

6 Bell, M.V., and D.R. Tocher. 2009. Biosynthesis of polyunsaturated fatty acids in aquatic ecosystems: general pathways and new directions. *In* Lipids in Aquatic Ecosystems. M.T. Arts, M. Brett and M. Kainz, editors. Springer-Verlag, New York, NY. 211–236.

7 Tocher, D.R. 2003. Metabolism and functions of lipids and fatty acids in teleost fish. *Rev. Fisheries Sci.* **11**: 107-184.

8 Tocher, D.R. 2010. Fatty acid requirements in ontogeny of marine and freshwater fish. *Aquacult. Res.* **41**: 717-732.

9 Hastings, N., M. Agaba, D.R. Tocher, M.J. Leaver, J.R. Dick, J.R. Sargent and A.J. Teale. 2001. A vertebrate fatty acid desaturase with Δ5 and Δ6 activities. *Proc. Natl. Acad. Sci. USA* **98**: 14304-14309.

10 Agaba, M., D.R. Tocher, C. Dickson, J.R. Dick and A.J. Teale. 2001. A zebrafish cDNA encoding a multifunctional enzyme involved in the elongation of polyunsaturated, monounsaturated and saturated fatty acids. *Mar. Biotechnol*. **6**: 251-261.

11 Zheng, X., I. Seiliez, N. Hastings, D.R. Tocher, S. Panserat, C.A. Dickson, P. Bergot and A.J. Teale. 2004. Characterisation and comparison of fatty acyl Δ6 desaturase cDNAs from freshwater and marine teleost fish species. *Comp. Biochem. Physiol*. **139***B*: 269-279.

12 Agaba, M.K., D.R. Tocher, C.A. Dickson, X. Zheng, J.R. Dick and A.J. Teale. 2005. Cloning and functional characterisation of polyunsaturated fatty acid elongases from marine and freshwater teleost fish. *Comp. Biochem. Physiol*. **142***B*: 342-352.

13 Hastings, N., M.K. Agaba, D.R. Tocher, X. Zheng, C.A. Dickson, J.R. Dick and A.J. Teale. 2005. Molecular cloning and functional characterization of fatty acyl desaturase and elongase cDNAs involved in the production of eicosapentaenoic and docosahexaenoic acids from α-linolenic acid in Atlantic salmon (*Salmo salar*). *Mar. Biotechnol*. **6**: 463-474.

14 Zheng, X., D.R. Tocher, C.A. Dickson, J.R. Dick, J.G. Bell and A.J. Teale. 2005. Highly unsaturated fatty acid synthesis in vertebrates: new insights with the cloning and characterisation of a Δ6 desaturase of Atlantic salmon. *Lipids* **40**: 13-24.

15 Tocher, D.R., X. Zheng, C. Schlechtriem, N. Hasting, J.R. Dick and A.J. Teale. 2006. Highly unsaturated fatty acid synthesis in marine fish: cloning, functional characterization, and nutritional regulation of fatty acyl Δ6 desaturase of Atlantic cod (*Gadus morhua* L.). *Lipids* **41**: 1003-1016.

16 González-Rovira, A., G. Mourente, X. Zheng, D.R. Tocher and C. Pendón. 2009. Molecular and functional characterization and expression analysis of a Δ6 fatty acyl desaturase cDNA of European sea bass (*Dicentrarchus labrax* L.). *Aquaculture* **298**: 90-100.

17 Monroig, Ó., J. Rotllant, E. Sánchez, J.M. Cerdá-Reverter and D.R. Tocher. 2009. Expression of long-chain polyunsaturated fatty acid (LC-PUFA) biosynthesis genes during zebrafish *Danio rerio* early embryogenesis. *Biochim. Biophys. Acta* **1791**: 1093-1101.

18 Morais, S., Ó. Monroig, X. Zheng, M.J Leaver and D.R. Tocher. 2009. Highly unsaturated fatty acid synthesis in Atlantic salmon: characterization of Elovl5- and Elovl2-like elongases. *Mar. Biotechnol*. **11**: 627–639.

19 Zheng, X., Z. Ding, Y. Xu, Ó. Monroig, S. Morais and D.R. Tocher. Physiological roles of fatty acyl desaturase and elongase in marine fish: Characterisation of cDNAs of fatty acyl Δ6 desaturase and Elovl5 elongase of cobia (*Rachycentron canadum*). *Aquaculture* **290**: 122-131.

20 Gregory, M., V.H.L. See, R.A. Gibson and K.A. Schuller. 2010. Cloning and functional characterisation of a fatty acyl elongase from southern bluefin tuna (*Thunnus maccoyii*). *Comp. Biochem. Physiol*. **155***B*: 178–185.

21 Mohd-Yusof, N.Y., Ó. Monroig, A. Mohd-Adnan, K.L. Wan and D.R. Tocher. 2010. Investigation of highly unsaturated fatty acid metabolism in the Asian sea bass, *Lates calcarifer*. *Fish Physiol. Biochem*. **3**: 827–843.

22 Monroig, Ó., X. Zheng, S. Morais, M.J. Leaver, J.B. Taggart and D.R. Tocher. 2010. Multiple genes for functional Δ6 fatty acyl desaturases (Fad) in Atlantic salmon (*Salmo salar* L.): Gene and cDNA characterization, functional expression, tissue distribution and nutritional regulation. *Biochim. Biophys. Acta* **1801**: 1072-1081.

23 Monroig Ó., J. Rotllant, J.M. Cerdá-Reverter, J.R. Dick, A. Figueras and D.R. Tocher. 2010. Expression and role of Elovl4 elongases in biosynthesis of very long-chain fatty acids during zebrafish *Danio rerio* early embryonic development. *Biochim. Biophys. Acta* **1801**: 1145-1154.

24 Carmona-Antoñanzas, G., Ó. Monroig, J.R. Dick, A. Davie and D.R. Tocher. 2011. Biosynthesis of very long-chain fatty acids (C > 24) in Atlantic salmon: Cloning, functional characterisation, and tissue distribution of an Elovl4 elongase. *Comp. Biochem. Physiol.* **159***B*: 122-129.

25 Monroig, Ó., K. Webb, L. Ibarra-Castro, G.J. Holt and D.R. Tocher. 2011. Biosynthesis of long-chain polyunsaturated fatty acids in marine fish: Characterization of an Elovl4-like elongase from cobia *Rachycentron canadum* and activation of the pathway during early life stages. *Aquaculture* **312**: 145–153.

26 Morais, S., G. Mourente, A. Ortega, J.A. Tocher and D.R. Tocher. 2011. Expression of fatty acyl desaturase and elongase genes, and evolution of DHA:EPA ratio during development of Atlantic bluefin tuna (*Thunnus thynnus* L.). *Aquaculture* **313**: 129-139.

27 Santigosa, E., F. Geay, T. Tonon, H. Le Delliou, H. Kuhl, R. Reinhardt, L. Corcos, C. Cahu, J.L. Zambonino-Infante and D. Mazurais. 2011. Cloning, tissue expression analysis, and functional characterization of two Δ6-desaturase variants of sea bass (*Dicentrarchus labrax* L.). *Mar. Biotechnol.* **13**: 22–31.

28 Monroig, Ó., S. Wang L. Zhang C. You, D.R. Tocher and Y. Li. 2012. Elongation of long-chain fatty acids in rabbitfish *Siganus canaliculatus*: Cloning, functional characterisation and tissue distribution of Elovl5- and Elovl4-like elongases. *Aquaculture* **350-353**: 63–70.

29 Tanomman, S., M. Ketudat-Cairns, A. Jangprai and S. Boonanuntanasarn. 2013. Characterization of fatty acid delta-6 desaturase gene in Nile tilapia and heterogenous expression in *Saccharomyces cerevisiae*. *Comp. Biochem. Physiol*. **166***B*: 148-156.

30 Monroig, Ó., D.R. Tocher, F. Hontoria and J.C. Navarro. 2013. Functional characterisation of a Fads2 fatty acyl desaturase with Δ6/Δ8 activity and an Elovl5 with C16, C18 and C20 elongase activity in the anadromous teleost meagre (*Argyrosomus regius*). *Aquaculture* **412-413**: 14–22.

31 Xie, D., F. Chen, S. Lin, S. Wang, C. You, Ó. Monroig, D.R. Tocher and Y. Li. 2014. Cloning, functional characterization and nutritional regulation of Δ6 fatty acyl desaturase in the herbivorous euryhaline teleost *Scatophagus argus*. *PLoS One* **9**: e90200.

32 Castro, L.F.C., Ó Monroig, M.J. Leaver, J. Wilson, I. Cunha and D.R. Tocher. 2012 Functional desaturase Fads1 (Δ5) and Fads2 (Δ6) orthologues evolved before the origin of jawed vertebrates. *PLoS One* **7**: e31950.

33 Carmona-Antoñanzas, G., D.R. Tocher, J.B. Taggart and M.J. Leaver. 2013. An evolutionary perspective on Elovl5 fatty acid elongase: comparison of Northern pike and duplicated paralogs from Atlantic salmon. *BMC Evolutionary Biol.* **13**: 85.

34 Tacon, A.G.J., M. Metian, G.M. Turchini and S.S. DeSilva. 2010. Responsible aquaculture and trophic level implications to global fish supply. *Rev. Fish. Sci.* **18**: 94–105.

35 Guillou, H., D. Zadravec, P.G.P. Martin and A. Jacobsson. 2010. The key roles of elongases and desaturases in mammalian fatty acid metabolism: Insights from transgenic mice. *Prog. Lipid Res.* **49**: 186-199.

36 Martínez-Palacios, C.A., M.G. Ríos-Duran, J. Fonseca-Madrigal M. Toledo-Cuevas, A. Sotelo Lopez and L.G. Ross. 2008. Developments in the nutrition of *Menidia estor* Jordan 1880. *Aquacult. Res*. **39**: 738-747.

37 Martínez-Palacios, C.A., E. Barriga-Tovar, J.F. Taylor, M.G. Ríos-Duran and L.G. Ross. 2002. Effect of temperature on growth and survival of *Chirostoma estor estor*, Jordan 1879, monitored using a simple video technique for remote measurement of length and mass of larval and juvenile fishes. *Aquaculture* **209**: 369-377.

38 Martínez-Palacios, C.A., I.S. Racotta, M.G. Ríos-Duran, E. Palacios, M. Toledo-Cuevas and L.G. Ross. 2006. Advances in applied research for the culture of Mexican silversides (*Chirostoma*, Atherinopsidae). *Biocell* **30**: 137-148.

39 Martínez-Palacios, C.A., L. Ambriz-Cervantes, M.G. Ríos-Duran, K.J. Jauncey and L.G. Ross. 2007. Dietary protein requirement of juvenile Mexican Silverside (*Chirostoma estor estor* Jordan 1879), a stomachless zooplanktophagous fish. *Aquaculture Nutr*. **13**: 304-310.

40 Barbour, C.D. 1973. The systematics and evolution of the genus *Chirostoma* Swainson (Pisces: Atherinidae). *Tulanne Stud. Zool. Bot*. **18**: 97-141.

41 Martínez-Palacios, C.A., J. Comas Morte, J.A. Tello-Ballinas, M. Toledo-Cuevas and L.G. Ross LG. The effects of saline environments on survival and growth of eggs and larvae of *Chirostoma estor estor* Jordan 1879 (Pisces: Atherinidae). *Aquaculture* **238**: 509-522.

42 Martínez-Palacios C.A., M.G. Ríos-Duran, A. Campos-Mendoza, M. Toledo-Cuevas, M.A. Aguilar-Valdez and L.G. Ross. 2003. Desarrollo tecnológico alcanzado en el cultivo del pez blanco de Pátzcuaro. *In* Historia y avances del cultivo de pescado blanco. Avances del cultivo de pescado blanco. P.M. Rojas-Carillo and D.F. Castellanos, editors. Pridsa Impresión. México, 169-190.

43 Fonseca-Madrigal, J., D. Pineda-Delgado, C.A. Martinez-Palacios, C. Rodriguez and D.R. Tocher. 2012. Effect of salinity on the biosynthesis of n-3 long-chain polyunsaturated fatty acids in silverside *Menidia estor*. *Fish Physiol. Biochem.* **38**:1047-1057.

44 Saitou, N. and M. Nei. 1987. The neighbor-joining method. A new method for reconstructing phylogenetic trees. *Mol. Biol. Evol*. **4**: 406-425.

45 Qiu, X., H.P. Hong and S.L. Mackenzie. 2001. Identification of a Δ4 fatty acid desaturase from *Thraustochytrium* sp. involved in biosynthesis of docosahexaenoic acid by heterologous expression in *Saccharomyces cerevisiae* and *Brassica juncea*. *J. Biol. Chem.* **276**: 31561-31566.

46 Ferdinandusse, S., S. Denis, C.W.T. van Roermund, R.J.A. Wanders and G. Dacremont. 2004. Identification of the peroxisomal-oxidation enzymes involved in the degradation of long-chain dicarboxylic acids. *J. Lipid Res.* **45**: 1104–1111.

47 Zheng, X., B.E. Torstensen, D.R. Tocher, J.R. Dick, R.J. Henderson and J.G. Bell. 2005. Environmental and dietary influences on highly unsaturated fatty acid biosynthesis and expression of fatty acyl desaturase and elongase genes in liver of Atlantic salmon (*Salmo salar*). *Biochim. Biophys. Acta* **1734**: 13–24.

48 Gregory, M., L.F. Cleland and M.J. James. 2013. Molecular basis for differential elongation of omega-3 docosapentaenoic acid by the rat Elovl5 and Elovl2. *J. Lipid Res.* **54**: 2851-2857.

49 Sasata, R.J., D.W. Reed, M.C. Loewen and P.S. Covello. 2004. Domain swapping localizes the structural determinants of regioselectivity in membrane-bound fatty acid desaturases of *Caenorhabditis elegans*. *J. Biol. Chem*. **279**: 39296–39302.

50 Song, L-Y., W-X. Lu, J. Hu, W-B. Yin, Y-H. Chen, B-L. Wang, R.R-C. Wang and Z-M. Hu. 2013. The role of C-terminal amino acid residues of a Δ6-fatty acid desaturase from blackcurrant. *Biochem. Biophys. Res. Commun*. **431**: 675-679.

51 Kurdrid, P., M. Sirijuntarut, S. Subudhi, S. Cheevadhanarak and A. Hongsthong. 2008. Truncation mutants highlight a critical role for the N- and C-termini of the *Spirulina* Δ6 desaturase in determining regioselectivity. *Mol. Biotechnol*. **38**: 203-209.

52 Betancur-R., R., R.E. Broughton, E.O. Wiley, K. Carpenter, J.A. López, C. Li, N.I. Holcroft, D. Arcila, M. Sanciangco, J.C. Cureton II, F. Zhang, T. Buser, M.A. Campbell, J.A. Ballesteros, A. Roa-Varon, S. Willis, W. Calvin Borden, T. Rowley, P.C. Reneau, D.J. Hough, G. Lu, T. Grande, G. Arratia and G. Ortí. 2013. The tree of life and a new classification of bony fishes. *PLoS Curr*. **18**: 1-45.

Figure legends

Fig. 1. Phylogenetic tree comparing the deduced amino acid (aa) sequence of the newly cloned *Chirostoma estor* fatty acyl desaturase (Fads) 2-like with Fads1- and Fads2-like desaturases from a variety of vertebrates. The tree was constructed using the neighbor-joining method (44) with MEGA4. The horizontal branch length is proportional to aa substitution per site. The numbers represent the frequencies with which the tree topology presented was replicated after 10,000 bootstrap iterations. All accession numbers are from GenBank database.

Fig. 2. Phylogenetic tree comparing the deduced amino acid (aa) sequence of the newly cloned *Chirostoma estor* elongase of very long-chain fatty acids (Elovl) with elongases Elovl2, Elovl4 and Elovl5 from a variety of vertebrates. The tree was constructed using the neighbor-joining method (44) with MEGA4. The horizontal branch length is proportional to aa substitution per site. The numbers represent the frequencies with which the tree topology presented was replicated after 10,000 bootstrap iterations. All accession numbers are from GenBank database.

Fig. 3. Functional characterization of the *Chirostoma estor* Fads2a and Fads2b desaturases in yeast (*Saccharomyces cerevisiae*). The fatty acid profiles of yeast transformed with pYES2-fadsa (panels A, C, E) and pYES2-fadsb (panels B, D, F) were determined after they were grown in presence of fatty acid substrates ("*") 18:3n-3 (A, B), 20:4n-3 (C, D), 22:5n-3 (E, F). Peaks 1-4 in all panels are the main endogenous fatty acids of *S. cerevisiae*, namely 16:0 (1), 16:1 isomers (2), 18:0 (3) and 18:1 isomers (4). Additionally peaks derived from exogenously added substrates and desaturated products are indicated accordingly. Vertical axis, FID response; horizontal axis, retention time.

Fig 4. Characterization of Δ8 desaturation activities of bifunctional Δ6/Δ5 Fads2b from *Chirostoma estor*. The fatty acid profiles of yeast transformed with pYES2-fadsb were determined after they were grown in presence of Δ8-desaturase substrates ("*"), namely 20:3n-3 (panel A) or 20:2n-6 (panel B). Peaks 1-4 in all panels are the main endogenous fatty acids of *S. cerevisiae*, namely 16:0 (1), 16:1 isomers (2), 18:0 (3) and 18:1 isomers (4). The substrates and their corresponding desaturated products are indicated. Peak indicated as "20:4" is a non-methylene interrupted FA ($^{\Delta6,11,14,17}$20:4 or $^{\Delta5,11,14,17}$20:4). Vertical axis, FID response; horizontal axis, retention time.

Fig. 5. Functional characterization of the of the newly cloned *Chirostoma estor* elongase of very long-chain fatty acids 5-like (Elovl5) in yeast (*Saccharomyces cerevisiae*). The fatty acid profiles of yeast transformed with pYES2 containing the coding sequence of Elovl5 as an insert, were determined after the yeast were grown in the presence of one of the exogenously added FA substrates ("*") 18:3n-3 (A), 18:4n-3 (B), 20:5n-3 (C) or 22:5n-3 (D). Peaks 1-4 in all panels are the main endogenous fatty acids of *S. cerevisiae*, namely 16:0 (1), 16:1 isomers (2), 18:0 (3) and 18:1 isomers (4). Additionally, peaks derived from exogenously added substrates and elongated products are indicated accordingly in panels A-D. Vertical axis, FID response; horizontal axis, retention time.

Fig. 6. Tissue distribution profile of *fads2a*, *fads2b* and *elovl5* transcripts in *Chirostoma estor* determined by quantitative real-time PCR (qPCR). Absolute copy numbers were quantified for each transcript and normalized by copy numbers of Elongation Factor 1α. Mean values are represented diagrammatically in logarithmic scale. Error bars are standard errors (n=3). The expressions of a gene in the different tissues studied that share the same letter are not significantly different (one-way ANOVA and Tukey's tests, $P<0.05$).

Fig 7. The biosynthesis pathway of long-chain polyunsaturated fatty acids from α-linolenic (18:3n-3) and linoleic (18:2n-6) acids in *Chirostoma estor*. Enzymatic activities shown in the scheme are predicted from heterologous expression in *Saccharomyces cerevisiae* of the Δ4 and Δ6/Δ5 desaturases (Fads2a and Fads2b, respectively) and the Elovl5-like elongase characterized in the present study.

Tables

Table 1. Functional characterization of the pike silverside (*Chirostoma estor*) desaturases Fads2a and Fads2b in *Saccharomyces cerevisiae*. Yeast *Saccharomyces cerevisiae* were transformed with pYES2-fadsa and pYES2-fadsb and grown in presence of Δ6 (18:3n-3 and 18:2n-6), Δ8 (20:3n-3 and 20:2n-6), Δ5 (20:4n-3 and 20:3n-6) and Δ4 (22:5n-3 and 22:4n-6) fatty acid (FA) substrates. Conversions were calculated according to the formula [individual product area/(all products areas+substrate area)]×100.

FA substrate	FA product	Conversion (%)		Activity
		Fads2a	Fads2b	
18:3n-3	18:4n-3	0	56.5	Δ6
18:2n-6	18:3n-6	0	25.2	Δ6
20:3n-3	20:4n-3	0	12.2*	Δ8
20:2n-6	20:3n-6	0	9.9*	Δ8
20:4n-3	20:5n-3	3.3	25.8	Δ5
20:3n-6	20:4n-6	0	11.6	Δ5
22:5n-3	22:6n-3	28.9	0	Δ4
22:4n-6	22:5n-6	10.3	0	Δ4

*Conversions of Δ8 substrates (20:3n-3 and 20:2n-6) by Fads2b include stepwise reactions due to multifunctional desaturation abilities. Thus, the conversions of the *C. estor* Fads2b on 20:3n-3 and 20:2n-6 include the Δ8 desaturation towards 20:4n-3 and 20:3n-6, respectively, and their subsequent Δ5 desaturations to 20:5n-3 and 20:4n-6, respectively.

Table 2. Functional characterization of the pike silverside (*Chirostoma estor*) elongase Elovl5 in *Saccharomyces cerevisiae*. Individual conversions were calculated according to the formula [individual product area/(all products areas+substrate area)]×100. Accumulated conversions were computed by summing the individual conversion for each particular product and also those for longer products.

FA substrate	FA product	% Individual conversion	% Accumulated conversion
18:3n-3	20:3n-3	35.6	41.1
	22:3n-3	5.5	5.5
18:2n-6	20:2n-6	4.9	5.2
	22:2n-6	0.3	0.3
18:4n-3	20:4n-3	27.2	60.2
	22:4n-3	33.0	33.0
18:3n-6	20:3n-6	27.2	27.2
	22:3n-6	0.0	0.0
20:5n-3	22:5n-3	87.1	89.6
	24:5n-3	2.5	2.5
20:4n-6	22:4n-6	53.8	54.8
	24:4n-6	1.0	1.0
22:5n-3	24:5n-3	1.9	1.9
22:4n-6	24:4n-6	0.6	0.6

FIGURE 1

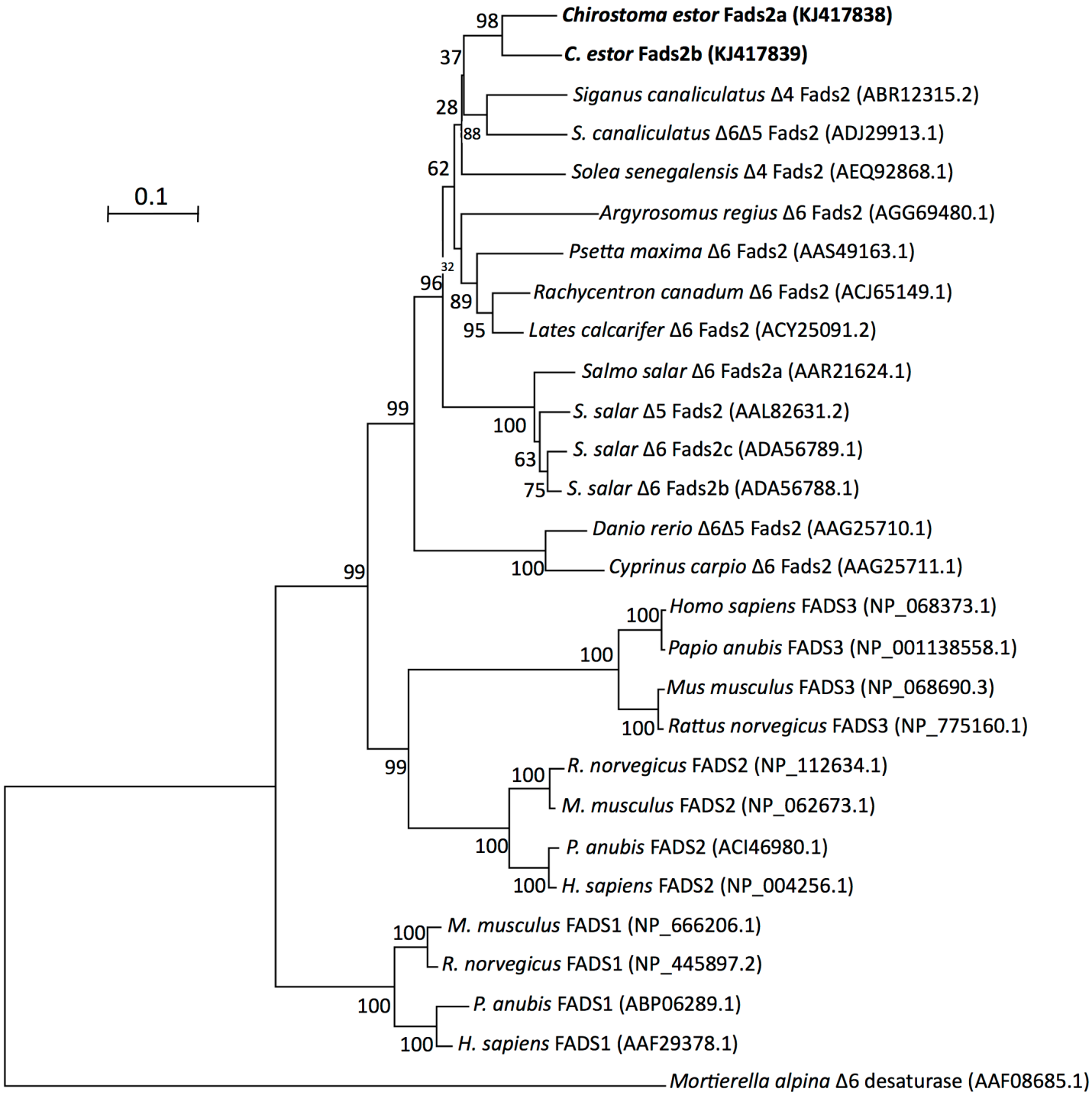

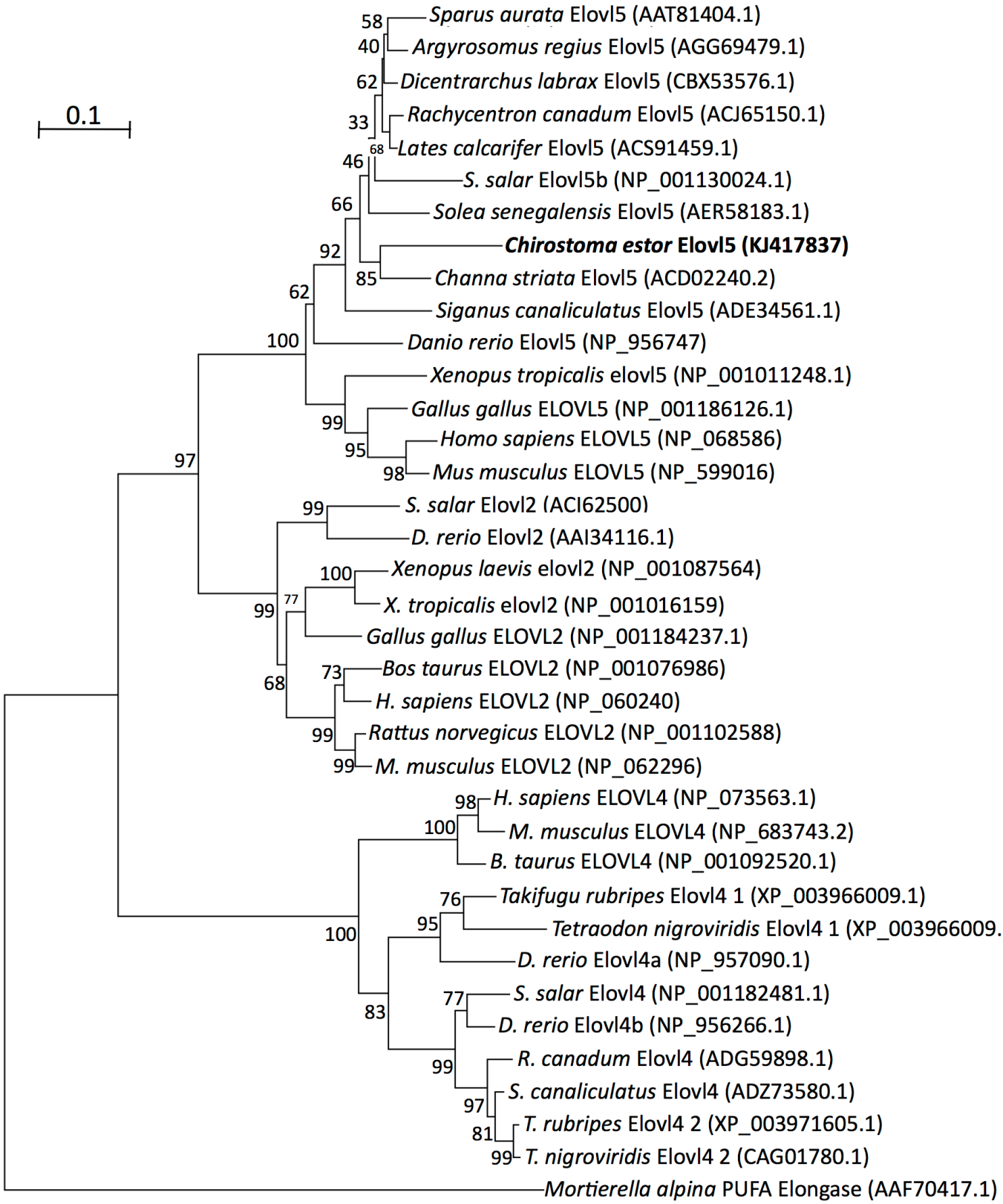
0.1
Sparus aurata Elovl5 (AAT81404.1)
Argyrosomus regius Elovl5 (AGG69479.1)
Dicentrarchus labrax Elovl5 (CBX53576.1)
Rachycentron canadum Elovl5 (ACJ65150.1)
Lates calcarifer Elovl5 (ACS91459.1)
S. salar Elovl5b (NP_001130024.1)
Solea senegalensis Elovl5 (AER58183.1)
Chirostoma estor Elovl5 (KJ417837)
Channa striata Elovl5 (ACD02240.2)
Siganus canaliculatus Elovl5 (ADE34561.1)
Danio rerio Elovl5 (NP_956747)
Xenopus tropicalis elovl5 (NP_001011248.1)
Gallus gallus ELOVL5 (NP_001186126.1)
Homo sapiens ELOVL5 (NP_068586)
Mus musculus ELOVL5 (NP_599016)
S. salar Elovl2 (ACI62500)
D. rerio Elovl2 (AAI34116.1)
Xenopus laevis elovl2 (NP_001087564)
X. tropicalis elovl2 (NP_001016159)
Gallus gallus ELOVL2 (NP_001184237.1)
Bos taurus ELOVL2 (NP_001076986)
H. sapiens ELOVL2 (NP_060240)
Rattus norvegicus ELOVL2 (NP_001102588)
M. musculus ELOVL2 (NP_062296)
H. sapiens ELOVL4 (NP_073563.1)
M. musculus ELOVL4 (NP_683743.2)
B. taurus ELOVL4 (NP_001092520.1)
Takifugu rubripes Elovl4 1 (XP_003966009.1)
Tetraodon nigroviridis Elovl4 1 (XP_003966009.1)
D. rerio Elovl4a (NP_957090.1)
S. salar Elovl4 (NP_001182481.1)
D. rerio Elovl4b (NP_956266.1)
R. canadum Elovl4 (ADG59898.1)
S. canaliculatus Elovl4 (ADZ73580.1)
T. rubripes Elovl4 2 (XP_003971605.1)
T. nigroviridis Elovl4 2 (CAG01780.1)
Mortierella alpina PUFA Elongase (AAF70417.1)

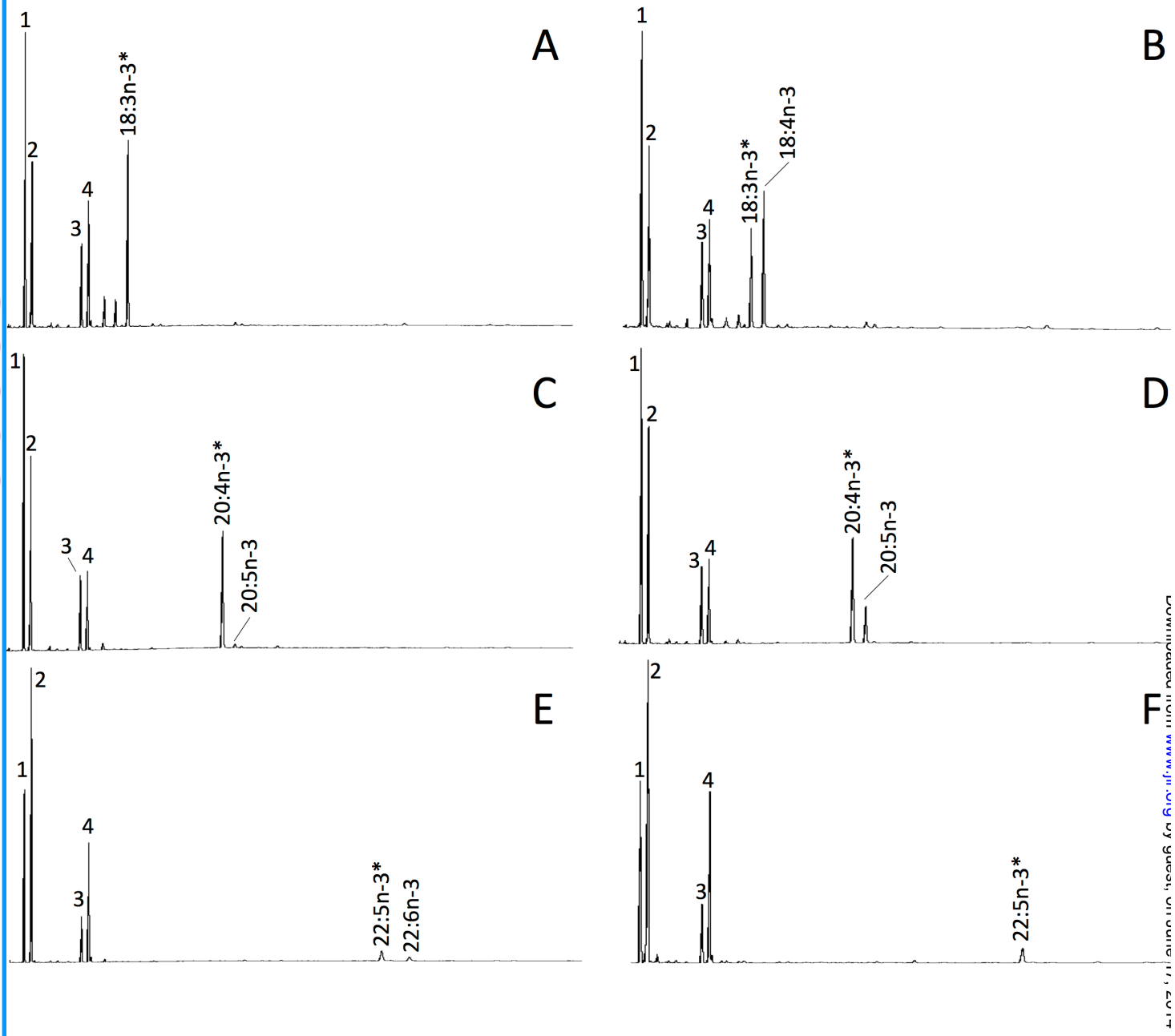

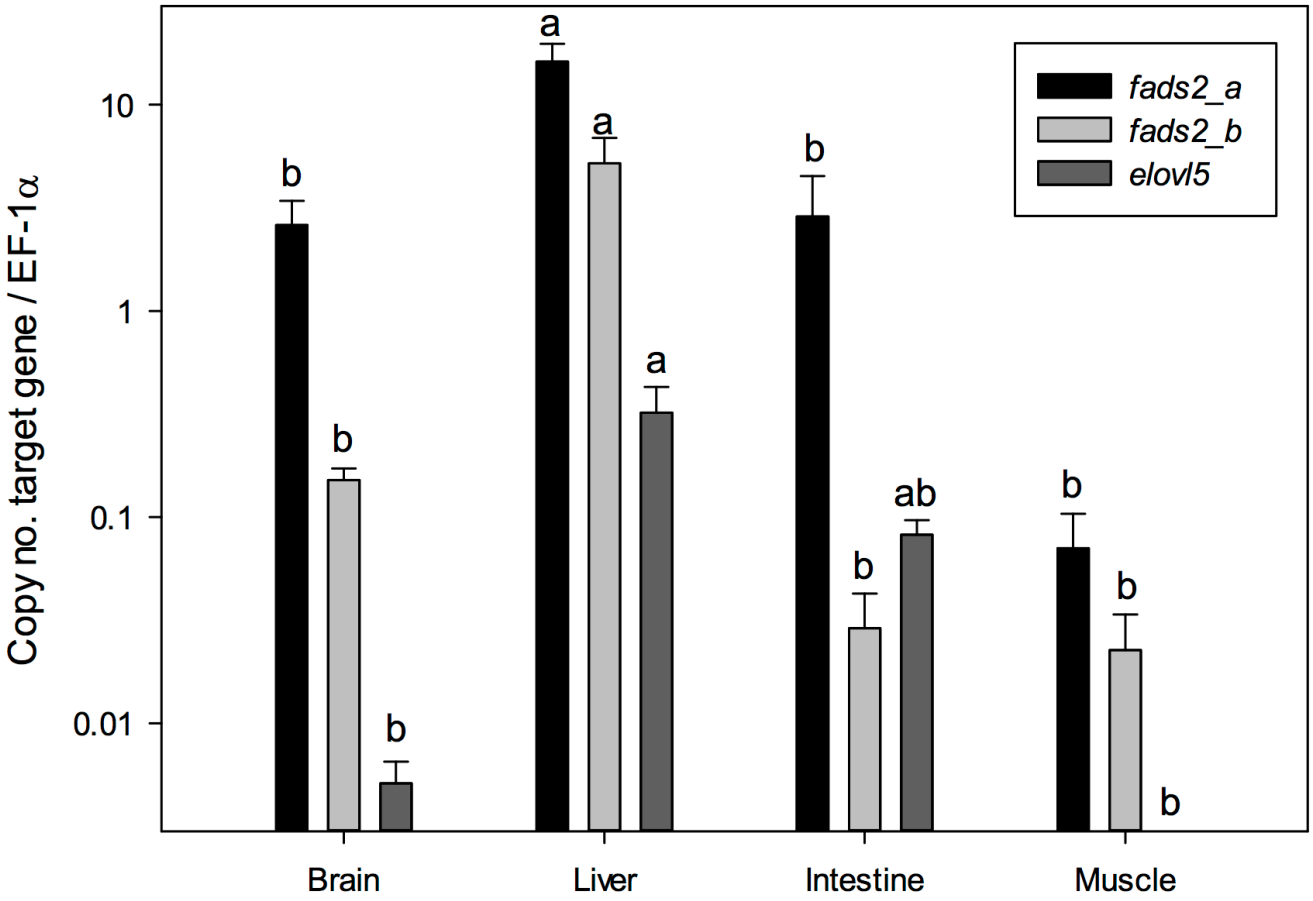
Copy no. target gene / EF-1α
10
1
0.1
0.01
fads2_a
fads2_b
elovl5
a
a
a
b
b
b
b
b
ab
b
b
b
Brain
Liver
Intestine
Muscle

FIGURE 7

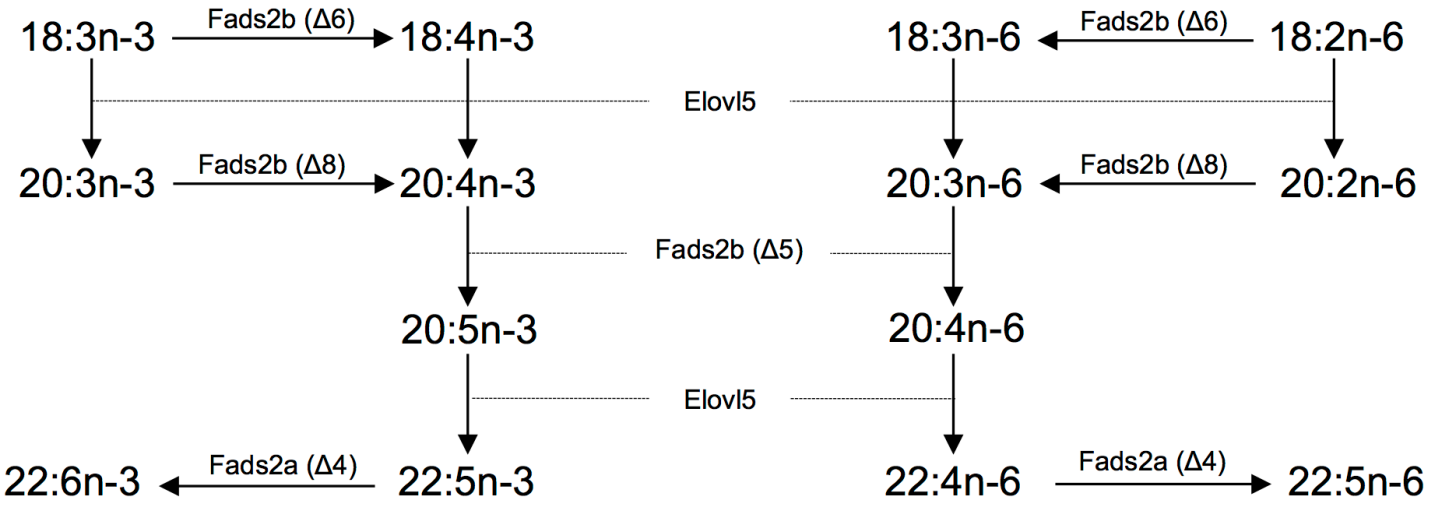
18:3n-3
Fads2b (Δ6)
18:4n-3
18:3n-6
Fads2b (Δ6)
18:2n-6
Elovl5
20:3n-3
Fads2b (Δ8)
20:4n-3
20:3n-6
Fads2b (Δ8)
20:2n-6
Fads2b (Δ5)
20:5n-3
20:4n-6
Elovl5
22:6n-3
Fads2a (Δ4)
22:5n-3
22:4n-6
Fads2a (Δ4)
22:5n-6